1.0

1.1

1.25 1.4 1.6

1.8 2.0 2.2 2.5 2.8 3.2 3.6 4.0 4.5 5.0 5.6

1 of 1

SAND93-0429C
Development of the FMT Chemical Transport Simulator:
Advective Transport Sensitivity to
Aqueous Density and Mineral Volume Fraction Coupled to Phase Compositions[*]

Craig F. Novak
Department 6119
Sandia National Laboratories
P.O. Box 5800
Albuquerque, New Mexico 87185-1320 USA

ABSTRACT

The Fracture-Matrix Transport (FMT) code couples saturated porous media advection and diffusion with mechanistic chemical models for speciation and interphase reactions. FMT is being developed to support actinide solubility and retardation studies for the Waste Isolation Pilot Plant (WIPP), a U.S. Department of Energy facility for demonstrating safe disposal of transuranic waste. Hydrologic studies of water-bearing units above the WIPP indicate double-porosity transport behavior in some locations, with groundwater concentrations ranging from potable to highly concentrated. Previously, FMT simulated such systems in two-dimensions on the continuum from advection- to diffusion-dominated, with a user-specified velocity field that allows double-porosity transport. However, aqueous density was assumed constant, and reactive minerals were assumed to occupy negligible volume. Both of these assumptions can be considered poor for evaporite systems, where large changes in porosity and aqueous density can result from high mineral solubilities. Therefore, further development of FMT has relaxed these restrictions, allowing aqueous density to vary with phase composition, and allowing void volume to change as minerals dissolve and precipitate. This paper describes the additional mathematical complexity required to simulate such systems. The sensitivity of advection-dominated transport to these variables is explored through an extended example.

Introduction

An overriding concern in the permanent disposal of nuclear waste is the isolation of hazardous radioactive elements from the geosphere. In the performance assessments of most repositories, the potential for mobilization of radioelements as dissolved or colloidal species in groundwaters is a driving scenario. A question of prime importance is often a variation of "If radioelements become mobilized by groundwaters, how much time will it take for these radioelements to reach the accessible environment?" Because regulatory time frames are often 10000 years or longer, it has been necessary to develop modeling capabilities to simulate these time frames.

This paper focuses on behavior of dissolved elements, deferring colloids to other works. If elements move with the groundwater, they are said to be unretarded, or conservative, tracers. Dissolved elements can migrate more slowly than the conservative tracers either because of *physical retardation*, caused by the geometry of the transport system, or because of *chemical retardation*, caused by chemical interactions between mobile and immobile phases. Migration of dissolved elements is calculated using computer codes of varying degrees of sophistication. The processes of advection, dispersion, and diffusion in the absence of chemical reaction are routinely calculated in two- and three-dimensions using standard methods from hydrology or petroleum engineering. Simulation of the more specialized double porosity systems, which couple advection-dominated and diffusion-dominated transport based on geometry, are also readily performed. These features constitute the physical portion of transport. The chemical phenomena that influence or govern transport include speciation (e.g., complexation, oxidation-reduction, etc.), ion exchange, adsorption, mineral dissolution/precipitation, and coprecipitation. Elements in the aqueous phase are mobile, while elements in or affixed to mineral phases are generally immobile.

Thus, chemical retardation is caused by mechanisms that remove radionuclides from the aqueous phase, thereby inhibiting transport. Nonlinear chemical effects are particularly important in environments with abrupt changes in chemical conditions, e.g., at the waste form boundary.

Most simulations of chemical transport in porous media assume one-way coupling of physical and chemical phenomena: advection, dispersion, and diffusion influence chemical compositions, but not the other way around. The development in this paper eliminates the need for this assumption. Mineral dissolution and precipitation are among the most important phenomena coupling physical transport to chemistry because they can alter the porosity available for the aqueous (transporting) phase. In enhanced oil recovery, mineral precipitation can reduce permeability (called formation damage) and thus reduce oil production rates. Within hazardous waste transport and depending on the system, porosity changes associated with mineral precipitation can be detrimental or beneficial to containment goals. If, as in a double porosity geometry, diffusion into secondary porosity is desirable for the physical retardation it provides, porosity reduction would be undesirable (Steefel and Lichtner, 1994). However, if diffusion is the dominant transport mechanism and chemical reactions decrease diffusion porosity, isolation effectiveness is enhanced. This work discusses the numerical developments required to rigorously model these phenomena. It is hoped that the FMT code with these developments can help address the lack of general and robust coupled geochemical and transport codes for nuclear waste applications (Neretnieks and Nyman, 1993).

FMT Development History

The Fracture-Matrix Transport (FMT) code has been designed to calculate the chemical changes in porous media associated with advection, dispersion, and

diffusion. Double porosity transport is of particular interest to the Waste Isolation Pilot Plant (WIPP), the current sponsor, and, as reflected in the name, this geometry has been emphasized, but FMT is a general two-dimensional transport simulator. FMT simulates transport within a rectangular domain using explicit finite differences coupled to a code-generated optimal set of chemical reactions among species specified by the user.

Development or maintenance of a thermodynamic data base is not within the charter for FMT. Consistent with this, any set of chemical data can be used as input data. However, because evaporite systems are of interest to the WIPP, the Pitzer model for brines (Pitzer, 1991) has been incorporated, as parameterized by Harvie et al. (1984) and extended by Felmy and Weare (1986) to cover large concentration ranges of the (pseudo-) elements Na, K, Mg, Ca, Cl, SO_4, CO_3, H, and OH, as well as restricted ranges for Pu(III), Am(III), and Th(IV) (Felmy et al., 1989; Felmy et al., 1990; Felmy and Rai, 1992; Roy et al., 1992). The equilibrium modeling capability of FMT is being continually updated as consistent Pitzer parameters become available for actinides. In addition, FMT simulations have been conducted (Novak and Nitsche, 1992) with data sets developed from IAEA and NEA actinide compilations (Fuger et al., 1992, Grenthe et al., 1992), and with data taken from the EQ3/6 data base (Wolery, 1979).

During the development of the code, before 2D and other capabilities were included, FMT was called GEOFLOW, and was used as the basis of a 1D, partial local equilibrium (PLE) transport code called KGEOFLOW (Sevougian, 1992). KGEOFLOW allows some reactions to be modeled with kinetic rate expressions while other reactions are modeled as at local equilibrium (LE). The choice of kinetics or equilibrium for each reaction is made by the user at run time, making the code very flexible. KGEOFLOW has been used to model the injection of concentrated acids to increase rock permeability in petroleum reservoirs (Sevougian

et al., 1992), and to demonstrate the formation of Liesegang rings caused by the interaction of nucleation, supersaturation, and advection/diffusion phenomena (Sevougian et al., 1993). These papers also demonstrate differences in the behavior of precipitation/dissolution waves between LE and PLE systems. Work in progress with KGEOFLOW is investigating the importance of intraaqueous redox kinetics on solute transport, a departure from most reaction/transport codes that use an overall system Eh. Plans exist to merge FMT and KGEOFLOW, to add the kinetic features of KGEOFLOW to the 2D and other features of FMT.

FMT has been applied to a fracture-matrix system demonstrating 2D retardation behavior with idealized and more realistic chemical models (Novak and Sevougian, 1992; Novak, 1993a). The degree of mathematical complexity needed to describe a fracture-matrix system based on flow parameters and system geometry is discussed by Novak (1993b) from an engineering perspective.

Current Extension

Recent development of FMT covers several of the features discussed in Novak (1993a). Of prime importance are:

(1) coupling aqueous density to aqueous composition,

(2) assigning realistic densities, and thus finite volumes, to mineral phases,

(3) allowing changes in phase volumes due to interphase mass transfer, and

(4) coupling phase volume changes to flow velocities.

In addition, local permeabilities are coupled to local porosities, a feature that in two dimensions could have a marked influence on preferred flow paths in heterogeneous systems (see for example Ortoleva et al., 1987a, 1987b).

Some fairly subtle complexities arise from allowing aqueous density to change as a function of composition, and allowing minerals to have volume. The salient feature is the change in phase volumes associated with chemical reactions,

because in general the density of the aqueous phase is not equal to the density of mineral phase(s) dissolving or precipitating. Because the sum of phase volumes must equal the bulk volume, these net volume expansions or contractions caused by chemical reactions result in local perturbations to the velocity profile. Indeed, in the limit of a purely diffusive transport system, mineral dissolution or precipitation should induce flow toward or away from the interphase reaction zone. A volume source will cause a local increase in system pressure, increasing velocity away from the source while a volume sink will cause a local decrease in system pressure, increasing velocity towards the source. Although this effect will likely be small in most cases, it does raise some interesting possibilities. A systematic way to calculate velocity field perturbations induced by phase volume changes is through the pressure equation, as discussed below.

Mathematical Development

The equations necessary for chemical transport include material balances for each element, an overall mass balance, a relationship between velocity and pressure, equations of state for aqueous density, and equations describing chemical reactions. This section documents the forms of these equations used within FMT, and provides an overview of the numerical methods used to solve the transport equations. The algorithm is a variation of that used to examine the production of a gas phase from mineral dissolution, and the attendant two-phase flow (Novak et al., 1990). FMT assumes equilibrium chemistry, and recent developments have not altered either the basic equations or the algorithms used for the chemical reaction equilibria. Details on these topics as they relate to FMT can be found in Novak (1993a) and Novak (1990); general details can be found in Denbigh (1981) and Smith and Missen (1982).

The two-dimensional transport equations for I chemical elements are

$$\frac{\partial}{\partial t}\left(\phi_1 C_1 + \phi_2 C_2\right) = \frac{\partial}{\partial x}\left(D\phi_1\frac{\partial C_1}{\partial x}\right) + \frac{\partial}{\partial y}\left(D\phi_1\frac{\partial C_1}{\partial y}\right) - \frac{\partial(C_1 u)}{\partial x} - \frac{\partial(C_1 v)}{\partial y} \qquad (1)$$

where $C_1(1,...,I)$ and $C_2(1,...,I)$ are vectors of element concentrations in the aqueous and mineral phases, respectively. The variables ϕ_1 and ϕ_2 are volume fractions of the aqueous and soluble solid phases, respectively. In arriving at Eq. 1, the effective diffusion/dispersion coefficient D was assumed to be the same for all species and thus can be used in the elemental material balances. An overall mass balance consistent with Eq. 1 is obtained from the dot product of Eq. 1 with the molecular weight vector **MW**. The diffusion terms cancel identically (Bird et al., 1960), giving

$$\frac{\partial}{\partial t}\left(\phi_1 \rho_1 + \phi_2 \rho_2\right) + \frac{\partial(\rho_1 u)}{\partial x} + \frac{\partial(\rho_1 v)}{\partial y} = 0 \qquad (2)$$

where the density of the jth phase is given by $\rho_j \equiv \sum_{i=1}^{I} MW_i C_{ij}$. Note that ρ_2 is a weighted average of individual mineral densities. Darcy's law is assumed for relating the aqueous velocity to the pressure gradient, and gravity effects are ignored:

$$u = -\frac{k}{\mu_1}\frac{\partial P}{\partial x} \qquad\qquad v = -\frac{k}{\mu_1}\frac{\partial P}{\partial y} \qquad (3)$$

(The system is currently considered isotropic, although there is nothing in the formulation that precludes anisotropy.) The overall force balance on the system, the "pressure equation," is thus

$$\frac{\partial}{\partial t}\left(\phi_1 \rho_1 + \phi_2 \rho_2\right) - \frac{\partial}{\partial x}\left(\frac{k\rho_1}{\mu_1}\frac{\partial P}{\partial x}\right) - \frac{\partial}{\partial y}\left(\frac{k\rho_1}{\mu_1}\frac{\partial P}{\partial y}\right) = 0 \qquad (4)$$

Here, the time derivative represents accumulation of total mass, which can be accomplished both through changing phase porosities and through changing phase densities.

Finite Difference Approximation to the Pressure Equation

Transport is calculated within FMT by solving time-explicit finite-difference analogs of the equations 1, 3 and 4 (see for example Peaceman, 1977), given as Eqs. 5, 6, and 7, respectively. Eqs. 5a and 5b recognize the decoupling between the aqueous (transporting) and the mineral (nontransporting) phases, showing that the mineral concentrations change only during the chemical reaction step (see Novak et al., 1991)

$$\frac{\left(\phi_1 C_1\right)_{ij}^{n+1} - \left(\phi_1 C_1\right)_{ij}^{n}}{\Delta t} =$$

$$\frac{(D\phi_1)_{i+1/2j}^{n}[C_{1i+1j}^{n} - C_{1ij}^{n}]}{\frac{1}{2}\Delta x_i(\Delta x_{i+1} + \Delta x_i)} - \frac{(D\phi_1)_{i-1/2j}^{n}[C_{1ij}^{n} - C_{1i-1j}^{n}]}{\frac{1}{2}\Delta x_i(\Delta x_i + \Delta x_{i-1})}$$

$$+ \frac{(D\phi_1)_{ij+1/2}^{n}[C_{1ij+1}^{n} - C_{1ij}^{n}]}{\frac{1}{2}\Delta y_j(\Delta y_{j+1} + \Delta y_j)} - \frac{(D\phi_1)_{ij-1/2}^{n}[C_{1ij}^{n} - C_{1ij-1}^{n}]}{\frac{1}{2}\Delta y_j(\Delta y_j + \Delta y_{j-1})}$$

$$- \frac{u_{i+1/2j}^{n+1}C_{1i+1/2j}^{n} - u_{i-1/2j}^{n+1}C_{1i-1/2j}^{n}}{\Delta x_i} - \frac{v_{ij+1/2}^{n+1}C_{1ij+1/2}^{n} - v_{ij-1/2}^{n+1}C_{1ij-1/2}^{n}}{\Delta y_j} \qquad (5a)$$

$$\frac{\left(\phi_2 C_2\right)_{ij}^{n+1} - \left(\phi_2 C_2\right)_{ij}^{n}}{\Delta t} = 0 \qquad (5b)$$

$$u_{i+1/2j} = -\left(\frac{k}{\mu_1}\right)_{i+1/2j}\frac{P_{i+1j} - P_{ij}}{\frac{1}{2}(\Delta x_{i+1} + \Delta x_i)} \qquad v_{ij+1/2} = -\left(\frac{k}{\mu_1}\right)_{ij+1/2}\frac{P_{ij+1} - P_{ij}}{\frac{1}{2}(\Delta y_{j+1} + \Delta y_j)}$$

$$u_{i-1/2j} = -\left(\frac{k}{\mu_1}\right)_{i-1/2j}\frac{P_{ij} - P_{i-1j}}{\frac{1}{2}(\Delta x_i + \Delta x_{i-1})} \qquad v_{ij-1/2} = -\left(\frac{k}{\mu_1}\right)_{ij-1/2j}\frac{P_{ij} - P_{ij-1j}}{\frac{1}{2}(\Delta y_j + \Delta y_{j-1})} \qquad (6)$$

$$\frac{\left(\phi_1\rho_1 + \phi_2\rho_2\right)_{ij}^{n+1} - \left(\phi_1\rho_1 + \phi_2\rho_2\right)_{ij}^{n}}{\Delta t} =$$

$$\frac{\left(\frac{k\rho_1}{\mu_1}\right)^{n+1}_{i+1/2j}[P^{n+1}_{i+1j} - P^{n+1}_{ij}]}{\frac{1}{2}\Delta x_i(\Delta x_{i+1} + \Delta x_i)} - \frac{\left(\frac{k\rho_1}{\mu_1}\right)^{n+1}_{i-1/2j}[P^{n+1}_{ij} - P^{n+1}_{i-1j}]}{\frac{1}{2}\Delta x_i(\Delta x_i + \Delta x_{i-1})} +$$

$$\frac{\left(\frac{k\rho_1}{\mu_1}\right)^{n+1}_{ij+1/2}[P^{n+1}_{ij+1} - P^{n+1}_{ij}]}{\frac{1}{2}\Delta y_j(\Delta y_{j+1} + \Delta y_j)} - \frac{\left(\frac{k\rho_1}{\mu_1}\right)^{n+1}_{ij-1/2}[P^{n+1}_{ij} - P^{n+1}_{ij-1}]}{\frac{1}{2}\Delta y_j(\Delta y_j + \Delta y_{j-1})} \tag{7}$$

Values on half-nodes are required for diffusion coefficients, aqueous viscosity and density, porosity, and permeability, yet these are undefined. As a first approximation, the viscosity is assumed to be constant, and the diffusion coefficient and porosity are found through interpolation (Oran and Boris, 1987). Aqueous density is upwinded, that is, the half-node value is set equal to the values in the grid block from which the aqueous phase is flowing, e.g.,

$$\left(\rho_1\right)^{n+1}_{i+1/2j} \equiv \begin{cases} \left(\rho_1\right)^{n+1}_{ij} & \text{for } P^{n+1}_{i+1j} \leq P^{n+1}_{ij} \\ \left(\rho_1\right)^{n+1}_{i+1j} & \text{for } P^{n+1}_{i+1j} > P^{n+1}_{ij} \end{cases} \tag{8}$$

However, this implies that the direction of flow is known, which is not necessarily true in all cases. Thus, values for coefficients will change when calculated flow directions are different from those initially assumed.

The transient pressure equation, Eq. 7, is solved using values for physical properties at the known time level n, and calculating pressures at time level n+1. At the start of a transport simulation, the accumulation term, i.e., the left-hand side, of Eq. 7 is unknown because of the explicit dependence on chemical reactions. Therefore, this is approximated as zero initially, and thus the steady-state analog to Eq. 7 is solved first. The pressures calculated are used to determine velocities, Eq. 6, and to transport concentrations, Eq. 5. These preliminary overall concentrations are speciated to determine provisional concentrations for time n+1. These provisional concentrations, along with associated phase densities and porosities, are

used to determine a better approximation to the accumulation term in Eq. 7, as given by

$$\frac{\left(\phi_1\rho_1 + \phi_2\rho_2\right)_{ij}^{n+1} - \left(\phi_1\rho_1 + \phi_2\rho_2\right)_{ij}^{n}}{\Delta t} = \frac{\left[(1-\phi_2-\phi_p)\rho_1\right]_{ij}^{n+1} - \left[\phi_1\rho_1\right]_{ij}^{n} + \left[\phi_2\rho_2\right]_{ij}^{n+1} - \left[\phi_2\rho_2\right]_{ij}^{n}}{\Delta t}$$

$$- \left\{ \frac{(D\phi_1)_{i+1/2j}^{n}[C_{1i+1j}^{n} - C_{1ij}^{n}]}{\frac{1}{2}\Delta x_i(\Delta x_{i+1} + \Delta x_i)} - \frac{(D\phi_1)_{i-1/2j}^{n}[C_{1ij}^{n} - C_{1i-1j}^{n}]}{\frac{1}{2}\Delta x_i(\Delta x_i + \Delta x_{i-1})} \right.$$

$$\left. + \frac{(D\phi_1)_{ij+1/2}^{n}[C_{1ij+1}^{n} - C_{1ij}^{n}]}{\frac{1}{2}\Delta y_j(\Delta y_{j+1} + \Delta y_j)} - \frac{(D\phi_1)_{ij-1/2}^{n}[C_{1ij}^{n} - C_{1ij-1}^{n}]}{\frac{1}{2}\Delta y_j(\Delta y_j + \Delta y_{j-1})} \right\} \cdot \mathbf{MW}^{\mathbf{T}} \qquad (9)$$

where all densities and concentrations on the right-hand-side are provisional (unconverged) values. Eq. 9 as written provides for successive substitution to approximate the source term, and also contains the constraint that the sum of phase volume fractions is unity, where ϕ_p is the nonreactive, or permanent, solid volume fraction.

The Nonnegativity Constraint

A useful constraint on time step size for this algorithm can be derived from Eq. 5. Negative concentrations are nonphysical, and frequently chemical equilibrium algorithms either set these concentrations to zero (which can wreak havoc with evaluation of global conservation of mass) or "bomb," both of which have serious consequences and implications for transport modeling. Inspection of Eq. 5 shows that, when $C_{jk}^{n} \leq 0 \; \forall j \; \forall k$, then C_{jk}^{n+1} is guaranteed nonnegative when

$$1 > \frac{\Delta t}{\phi_{ij}\Delta x_i}\left(\text{MAX}(0,u_{i+1/2j}) - \text{MIN}(0,u_{i-1/2j})\right) + \frac{\Delta t}{\phi_{ij}\Delta y_j}\left(\text{MAX}(0,v_{ij+1/2}) - \text{MIN}(0,v_{ij-1/2})\right)$$

$$+ \frac{2\Delta t}{\phi_{ij}\Delta x_i}\left(\frac{D_{i+1/2j}\,\phi_{i+1/2j}}{\Delta x_i + \Delta x_{i+1}} + \frac{D_{i-1/2j}\,\phi_{i-1/2j}}{\Delta x_{i-1} + \Delta x_i}\right) + \frac{2\Delta t}{\phi_{ij}\Delta y_j}\left(\frac{D_{ij+1/2}\,\phi_{ij+1/2}}{\Delta y_j + \Delta y_{j+1}} + \frac{D_{ij-1/2}\,\phi_{ij-1/2}}{\Delta y_{j-1} + \Delta y_j}\right) \qquad (9)$$

The terms containing MIN and MAX take flow direction into account using upwind differencing, as discussed earlier. Eq. 9, called for convenience the "nonnegativity

constraint," can be used as a guide to determine finite difference parameters such that negative concentrations cannot be produced in Eq. 5. For simple 1D transport with constant coefficients, Eq. 9 collapses to the familiar stability constraints on the analogous linear PDE's under finite differences: $\frac{D\Delta t}{\Delta x^2} < \frac{1}{2}$ for pure diffusive transport, and $\frac{u\Delta t}{\phi\Delta x} < 1$ for pure advective transport. Using a time step size greater than that specified by Eq. 9 does not force negative values for concentration, but it does generally lead to a nonphysical result. Eq. 9 is not sufficient to demonstrate stability, but serves as a useful guide.

Recently, a broad statement that "iteration between the hydrologic and chemical submodels [within a time step] is critical to accurate calculations" was put forth (Yeh and Tripathi, 1991). This statement is rather more general than is justifiable. Chemical transport results from intimate interaction between mobile and immobile phases, therefore, intimate coupling is required. But it is not important whether this interaction occurs as "iterations" within a time step (e.g., in implicit methods) or as time splitting with one call to the chemical module per time step (e.g., in explicit methods). Either approach can provide the interaction between chemical and hydrologic modules necessary to solve the problem, even though no "iteration" is technically occurring in the explicit methods. As Δt is increased in the implicit formulations, the number of iterations with the chemical module required per time step should also increase to achieve the necessary coupling. However, particularly for systems with dissolution/precipitation reactions, large time steps effectively prevent the mineral aqueous coupling necessary to describe the propagating dissolution/precipitation waves, and can provide increasingly inaccurate solutions. Indeed, in 1D scoping calculations, implicit methods resulted in less accurate solution of dissolution/precipitation systems for the same CPU time. Systems with continuous isotherms relating aqueous to, e.g., sorbed concentrations, may be less subject to these symptoms than dissolution/precipitation systems.

Nevertheless, it is important to provide adequate coupling between aqueous and mineral phases to allow the transport-controlling interphase reactions to occur and influence advection-dispersion behavior.

Advective Sensitivity

The importance of coupling porosity, mineral dissolution/precipitation, and transport in pure diffusive systems has been recognized, and initial examinations have been performed by Carnahan (1990) and Lichtner and Steefel (1994). The following section is a brief study examining the sensitivity of advective transport to changes in phase volumes as minerals dissolve and precipitate. One-dimensional simulations were used to simplify and emphasize these effects. The effects of changing porosity on permeabilities and dominant flow paths can be very important. Various correlations between porosity and permeability have been proposed (Reis and Acock, 1993). However, multi-dimensional numerical studies of porosity and permeability coupling are deferred to future works.

To estimate the relative importance of the effects of finite mineral volumes and composition-dependent aqueous phase density, consider the following static system. Assume a system with 1000 g H_2O and enough mineral to dissolve in that water to bring the system to saturation (assume congruous dissolution). The total initial and final volumes of this system are given by

$$V_i = \frac{1000 \text{ g } H_2O}{\rho_1(0)} + \frac{M_2^f}{\rho_2} \qquad V_f = \frac{1000 + M_2^f}{\rho_1(M_2^f)} \tag{10}$$

where ρ_2 is the solid phase density, $\rho_1(0)$ is the density of pure water, and $\rho_1(M_2^f)$ is the density of a solution of M_2^f grams of the solid dissolved in 1000 g pure water.

The percentage relative change in total volume calculated using these relationships

and a correlation between aqueous density and composition[*] is plotted for different mineral densities in Fig. 1. As shown, the net change in volume is less than 5% for minerals with densities of 2000 to 4000 kg/m^3, even up to high brine concentrations. For systems in which mineral volumes are assumed negligible, equivalent to ρ_2 approaching infinity, the total volume change can be as high as 15%. This effect is emphasized in going from dilute to very concentrated systems; the percentage total volume change for solutions with initial nonzero solute amounts can be found by ratio. Thus, the effects purely from volume changes associated with mass changing phase are expected to be small.

To examine transport sensitivity to volume changes associated with mass changing phase, a simple 1D advection-dominated transport problem with mineral dissolution/precipitation was run for four different sets of conditions. The transport problem was arbitrarily chosen with an initial condition of a halite-containing/halite-saturated column into which a nearly saturated $MgSO_4$(aq) solution was introduced, causing equilibrium dissolution and precipitation. This problem is not meant to be representative of any physical process, but was chosen merely to illustrate potential effects of including realistic phase volume descriptions in chemical transport simulators. The four scenarios differ in assumptions used for phase densities: the aqueous phase either has a constant density or a composition-dependent density; the mineral phases either occupy a negligible volume (densities approaching infinity) or occupy a realistic volume (realistic densities). Details for the simulations are given in Table 1.

---

[*] A best-fit linear correlation relating the density of NaCl solutions to the total dissolved Na and Cl in grams Na+Cl per liter solution, using 20°C data from Weast (1980), seemed adequate to approximate density/compostion behavior for purposes of this paper. The correlation

$$\rho_1 \text{ (g/l)} = 1000.96 \text{ (g/l)} + \frac{0.669963 \text{ (g/l)}}{\text{(g solute/liter solution)}} \times \text{TDS (g solute/liter solution)}$$

is linear with a correlation coefficient of R=0.9994.

In all simulations, the initial aqueous porosity ϕ_1 is 0.183, with an initial reactive mineral volume fraction of either 0.017 (when minerals have volume) or 0.0 (when minerals effectively have no volume). For variable ρ_1 and realistic mineral densities, results from the transport simulations with 20 and 40 nodes are shown in Figure 2, and illustrate the features of this system. The halite initially present dissolves in a sharp front at which bloedite precipitates, and bloedite in turn dissolves in a sharp front at which epsomite precipitates. The volume fraction occupied by soluble solids increases from 1.7% initially (halite) to about 3.0% (bloedite) to about 4.8% (epsomite), and finally is reduced to 0% as the epsomite dissolves. The agreement between the 40 node simulation (lines) and the 20 node simulation (symbols) indicates convergence of the numerical solution on the 40 node grid. The difference in the curvature of the tracer wave (fractional length $> \sim 0.60$) is caused by different values of numerical dispersion.

The incorporation and release of H_2O into/from mineral phases have a dramatic influence on aqueous tracer concentrations, as Fig. 3 demonstrates. The dissolution of epsomite;

$$MgSO_4 \bullet 7H_2O\text{(epsomite)} \leftrightarrow Mg^{2+} + SO_4^{2-} + 7H_2O$$
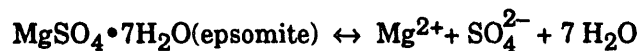
releases H_2O into the aqueous phase, reducing the normalized T(aq) concentration below unity. Downstream, at the bloedite dissolution-epsomite precipitation front, some of the H_2O is removed from the aqueous phase via

$$Na_2Mg(SO_4)_2 \bullet 4H_2O\text{(bloedite)} + 3H_2O \leftrightarrow MgSO_4 \bullet 7H_2O\text{(epsomite)} + 2Na^+ + SO_4^{2-}$$
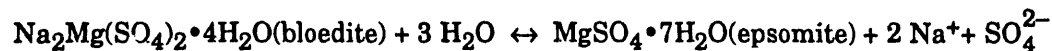
and also at the halite dissolution-bloedite precipitation front via the reaction

$$NaCl\text{(halite)} + Mg^{2+} + 2SO_4^{2-} + 4H_2O \leftrightarrow Na_2Mg(SO_4)_2 \bullet 4H_2O\text{(bloedite)} + 2Cl^-$$
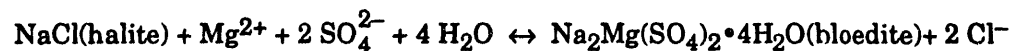
The combined sinks of water into the mineral phase concentrate T(aq) to about 1.2 times its injected concentration. Thus, the removal/addition of water from/to the

aqueous phase through mineral dissolution/precipitation reactions causes the stepped tracer concentration profile seen in Fig. 3. The gradual decrease in T(aq) concentration at the right end of the domain reflects the expected numerical dispersion in the tracer concentration profile. Also shown in this figure is the analytical solution corresponding to a tracer wave, at 1.22 times normalized concentration, for comparison of dispersion.

Mineral concentrations for the four different scenarios are shown in Figure 4. It is obvious from this figure that the volume effects have a small impact on the rate of dissolution/precipitation wave propagation in these advection-dominated systems.

Concluding Remarks

The FMT simulator now allows realistic representation of mineral volumes and aqueous phase densities, and couples changes in these properties to flow and transport. As anticipated, these features do not appear to be important in one-dimensional advection-dominated simulations. However, it has been shown how these features can be important in two- and three-dimensional simulations where changes in porosity can alter dominant flow paths in advection-dominated transport regions and can enhance or restrict diffusion-dominated transport. In addition, changes in porosity may be important in determining whether transport in regions of a particular system are diffusion-dominated or advection-dominated. The FMT code allows rigorous simulation of these phenomena as governed by equilibrium chemical reactions. Although the 2D implimentation in FMT was verified, time constraints did not allow presentation of 2D examples here. These effects will be examined in detail for future publications.

References

Bird, R. B., W. E. Stewart, and E. N. Lightfoot. 1960. *Transport Phenomena*. New York: John Wiley and Sons.

Carnahan, C.L. 1990. "Coupling of Precipitation-Dissolution Reactions to Mass Diffusion via Porosity Changes." Chapter 18 in D.C. Melchior and R.L. Bassett, eds. *Chemical Modeling in Aqueous Systems II*. American Chemical

Society Symposium Series, No. 416. Washington, D.C.: American Chemical Society.

Denbigh, K. 1981. *The Principles of Chemical Equilibrium*. Cambridge: Cambridge University Press.

Felmy, A.R., and D. Rai. 1992. "An Aqueous Thermodynamic Model for a High Valence 4:2 Electrolyte $Th^{4+}-SO_4^{2-}$ in the System $Na^+-K^+-Li^+-NH_4-SO_4-HSO_4-H_2O$ to High Concentration." *Journal of Solution Chemistry* vol. 21 #5: 407-423.

Felmy, A.R., D. Rai, and R.W. Fulton. 1990. "The Solubility of $AmOHCO_3(c)$ and the Aqueous Thermodynamics of the System $Na^+-Am^{3+}-HCO_3-OH^--H_2O$." *Radiochimica Acta* vol. 50: 193-240.

Felmy, A.R., D. Rai, J.A. Schramke, and J.L. Ryan. 1989. "The Solubility of Plutonium Hydroxide in Dilute Solution and in High-Ionic-Strength Chloride Brines." *Radiochimica Acta* vol. 48: 29-35.

Felmy, A.R., and J.H. Weare. 1986. "The Prediction of Borate Mineral Equilibria in Natural Waters: Application to Searles Lake, California." *Geochimica et Cosmochimica Acta* vol. 50: 2771-2783.

Fuger, J., I.L. Khodakovsky, E.I. Sergeyeva, V.A. Medvedev, and J.D. Navratil. 1992. *The Chemical Thermodynamics of Actinide Elements and Compounds: Part 12: The Actinide Aqueous Inorganic Complexes*. International Atomic Energy Agency: Vienna, Austria.

Grenthe, I., J. Fuger, R.J.M. Konings, R.J. Lemire, A.B. Muller, C. Nguyen-Trung, and H. Wanner. 1992. *Chemical Thermodynamics of Uranium*. Wanner, H, and I. Forest, eds. Elsevier Science Publishers: Amsterdam, The Netherlands.

Harvie, C.E., N. Møller, and J.H. Weare. 1984. "The Prediction of Mineral Solubilities in Natural Waters: The $Na-K-Mg-Ca-H-Cl-SO_4-OH-HCO_3-CO_3-CO_2-H_2O$ System to High Ionic Strength at 25°C." *Geochimica et Cosmochimica Acta* vol. 48: 723-751.

Neretnieks, I., and C. Nyman. 1993. "Use of Coupled Geochemical and Transport Calculations for Nuclear Waste Problems." in *High Level Radioactive Waste Management, Proceedings of the Foiurth Annual International Conference, Las Vegas, Nevada, April 26-30, 1993*. pp. 1533-1538.

Novak, C.F. 1993a. "Modeling Mineral Dissolution and Precipitation in Dual-Porosity Fracture-Matrix Systems." *Journal of Contaminant Hydrology* vol. 13: 91-115.

Novak, C.F. 1993b. "Transport Modeling in a Finite Fractured Rock Domain," in *Materials Research Society Symposium Proceedings. Volume 294. Scientific Basis for Nuclear Waste Management XVI*. C.G. Interrante and R.T. Pabalan, editors. Pittsburgh, Pennsylvania: Materials Research Society. Vol. 294, 831-838.

Novak, C.F., L.W. Lake, and R.S. Schechter. 1991. "Geochemical Modeling of Two Phase Flow with Interphase Mass Transfer." American *Institute of Chemical Engineers Journal*, vol. 37 #11: 1625-1633.

Novak, C.F., and S.D. Sevougian. 1993. "Propagation of Dissolution/Precipitation Waves in Porous Media," in *Migration and Fate of Pollutants in Soils and Subsoils. NATO ASI Series. Series G: Ecological Sciences, Vol. 32*. D. Petruzzelli and F.G. Helfferich, editors. Berlin, Germany: Springer-Verlag. Vol. 32, 275-307. Also published as SAND92-0364. Albuquerque, New Mexico: Sandia National Laboratories.

Oran, E. S., and J. P. Boris. 1987. *Numerical Simulation of Reactive Flows*. New York: Elsevier Publications.

Ortoleva, P., E. Merino, C. Moore and J. Chadam. 1987a. "Geochemical Self-Organization I: Reaction-Transport Feedbacks and Modeling Approach." *American Journal of Science* vol. 287: 979-1007.

Ortoleva, P., J. Chadam, E. Merino, and A. Sen. 1987b. "Geochemical Self-Organization II: The Reactive-Infiltration Instability." *American Journal of Science* vol. 287: 1008-1040.

Peaceman, D.W. 1977. *Fundamentals of Numerical Reservoir Simulation*. New York: Elsevier.

Pitzer, K.S. 1991. *Activity Coefficients in Electrolyte Solutions*. Boca Raton, Florida: CRC Press.

Reis, J.C., and A. Acock. 1993. "Permeability Reduction Models for the Precipitation of Inorganic Solids in Geologic Formations." *In Situ* submitted 1993.

Roy, R.N., K.M. Vogel, C.E. Good, W.B. Davis, L.N. Roy, D.A. Johnson, A.R. Felmy, and K.B. Pitzer. 1992. "Activity Coefficients in Electrolyte Mixtures: $HCl + ThCl_4 + H_2O$ for 5°–55°C." *Journal of Physical Chemistry* vol. 96: 11065-11072.

Sevougian, S.D. 1992. *Partial Local Equilibrium and the Propagation of Mineral Alteration Zones*. Doctoral Thesis, University of Texas at Austin. Ann Arbor, Michigan: University Microfilms.

Sevougian, S.D., L.W. Lake, and R.S. Schechter. 1992. "A New Geochemical Simulator to Design More Effective Sandstone Acidizing Treatments." SPE Paper 24780, presented at the 67th Annual Technical Conference and Exhibition of the Society of Petroleum Engineers, Washington, D.C., Oct. 4-7, 1992.

Sevougian, S.D., R.S. Schechter, and L.W. Lake. 1993. "Effect of Partial Local Equilibrium on the Propagation of Precipitation/Dissolution Waves." *Ind. Eng. Chem. Research* vol. 32 #10: 2281-2304.

Smith, W.R., and R.W. Missen. 1982. *Chemical Reaction Equilibrium Analysis: Theory and Algorithms*. New York: John Wiley and Sons.

Steefel, C.I., and P.C. Lichtner. 1994. "Diffusive Transport of a Reactive Hyperalkaline Fluid into a Marl Host Rock." *Geochimica et Cosmochimica Acta* submitted 1993.

Weast, R.C. 1980. *CRC Handbook of Chemistry and Physics* 60th ed. Chemical Rubber Publishing Company, Boca Raton, Florida.

Wolery, T.J. 1979. Calculation of Chemical Equilibrium Between Aqueous Solution and Minerals: the EQ3/6 Software Package. UCRL-52658. Livermore, California: Lawrence Livermore Laboratory.

Yeh, G. T., and V. S. Tripathi. 1991. "A Model for Simulating Transport of Reactive Multispecies Components: Model Development and Demonstration." *Water Resources Research* vol. 27: 3075-3094.

Table 1.   Parameters used for transport simulations.

Mineral Name	Chemical Formula	Molecular Weight, g/mole	Density, kg/m^3 (Weast, 1980)	Density to give negligible volume, kg/m^3
Halite	NaCl(s)	58.443	2165	1×10^7
Epsomite	$MgSO_4 \cdot 7H_2O(s)$	246.469	1677	1×10^7
Bloedite	$Na_2Mg(SO_4)_2 \cdot 4H_2O(s)$	334.461	2250	1×10^7

Concentrations

		Initial Condition	Injected Condition	when ρ_1=constant
Na	(molal)	6.085	0	-
Cl	(molal)	6.085	0	-
Mg	(molal)	0	2.666	-
SO4	(molal)	0	2.666	-
T(aq)	(molal)	0	1.011×10^{-6}	-
Ionic Strength	(molal)	6.08	10.7	-
Density	(kg/m^3)	1203	1185	1194

Numerical Integration Parameters

	20 nodes	40 nodes
Δx (m)	0.005	0.0025
Δt (sec/PV*)	4500/0.025	2250/0.0125
u (m/s)	1×10^{-7}	1×10^{-7}
D* (numerical) (m^2/s)	$2.28x^{-10}$	1.14×10^{-10}
NPe(numerical)	220	481

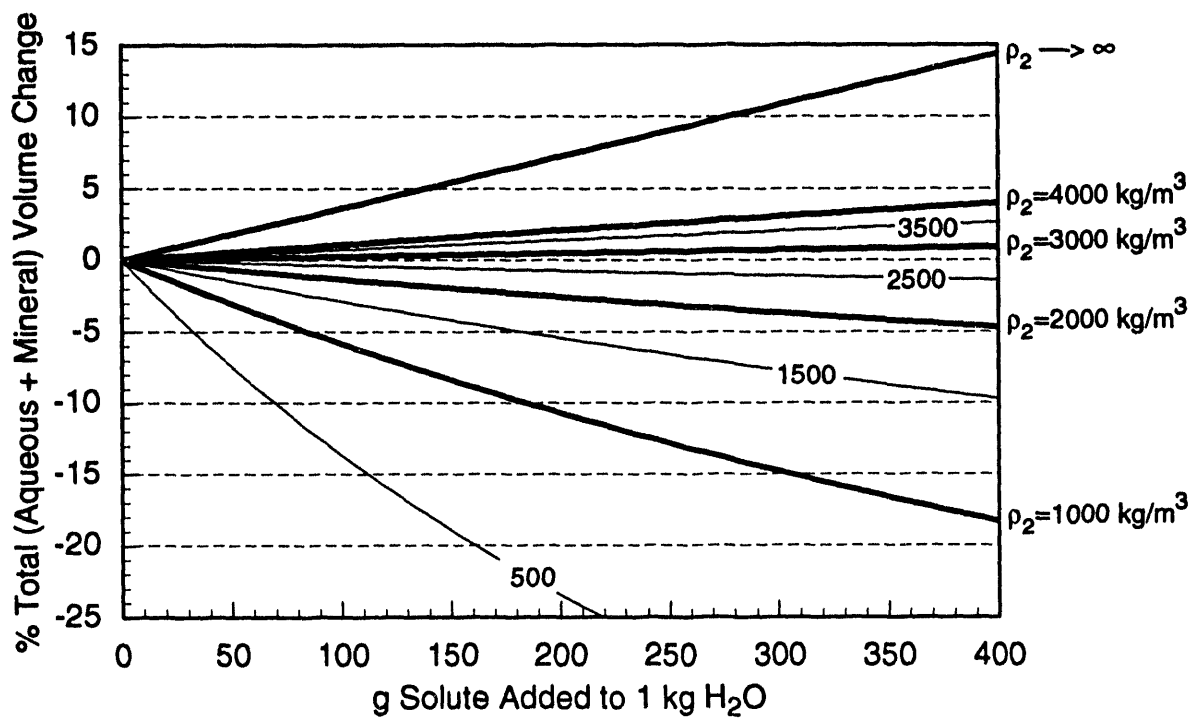*   PV, pore volumes, is a dimensionless time given by $PV=\dfrac{ut}{L\phi}$

Figure 1. Calculated change in total (aqueous+mineral) volume upon mineral dissolution, see Eq. 10, parameterized for a range of mineral densities.
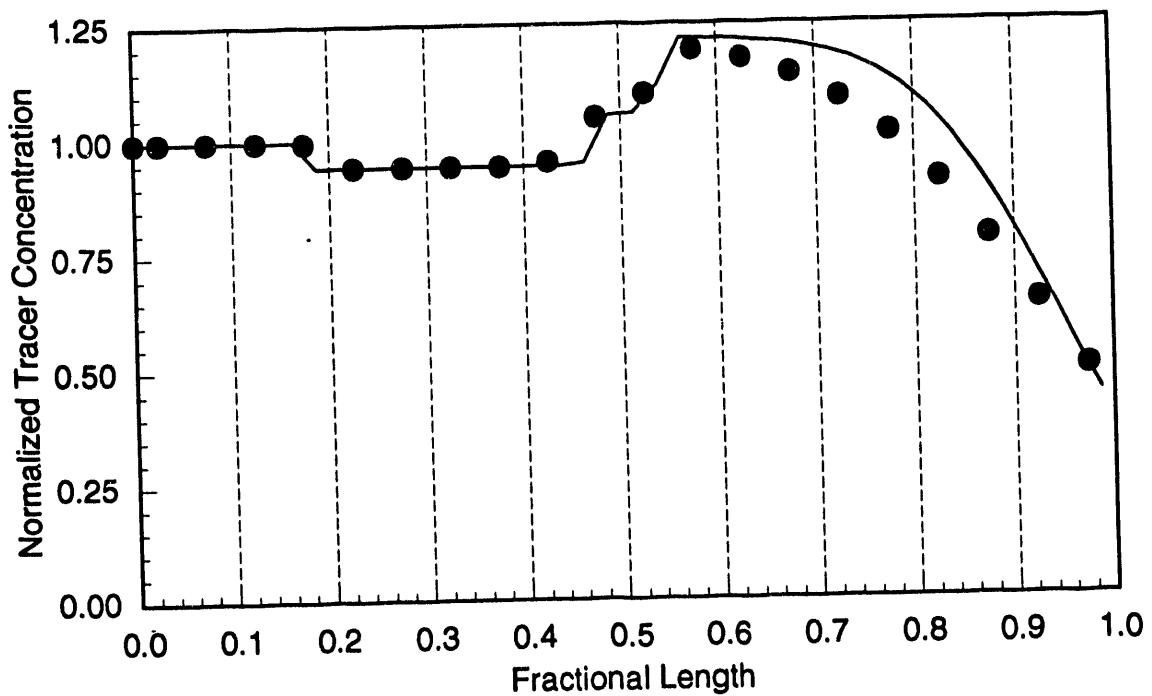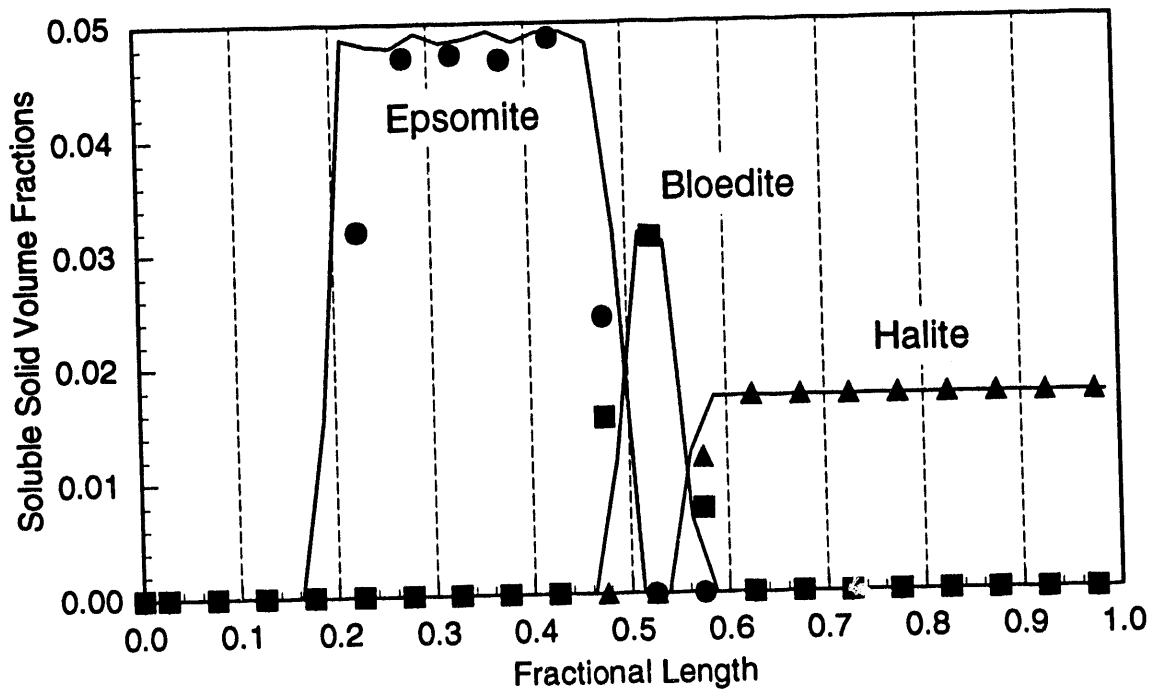
Figure 2. Wave behavior of illustrative problem, and comparison of 20-node (symbols) and 40-node (lines) simulations including all volume effects at t=1.8 × 10⁵ seconds.
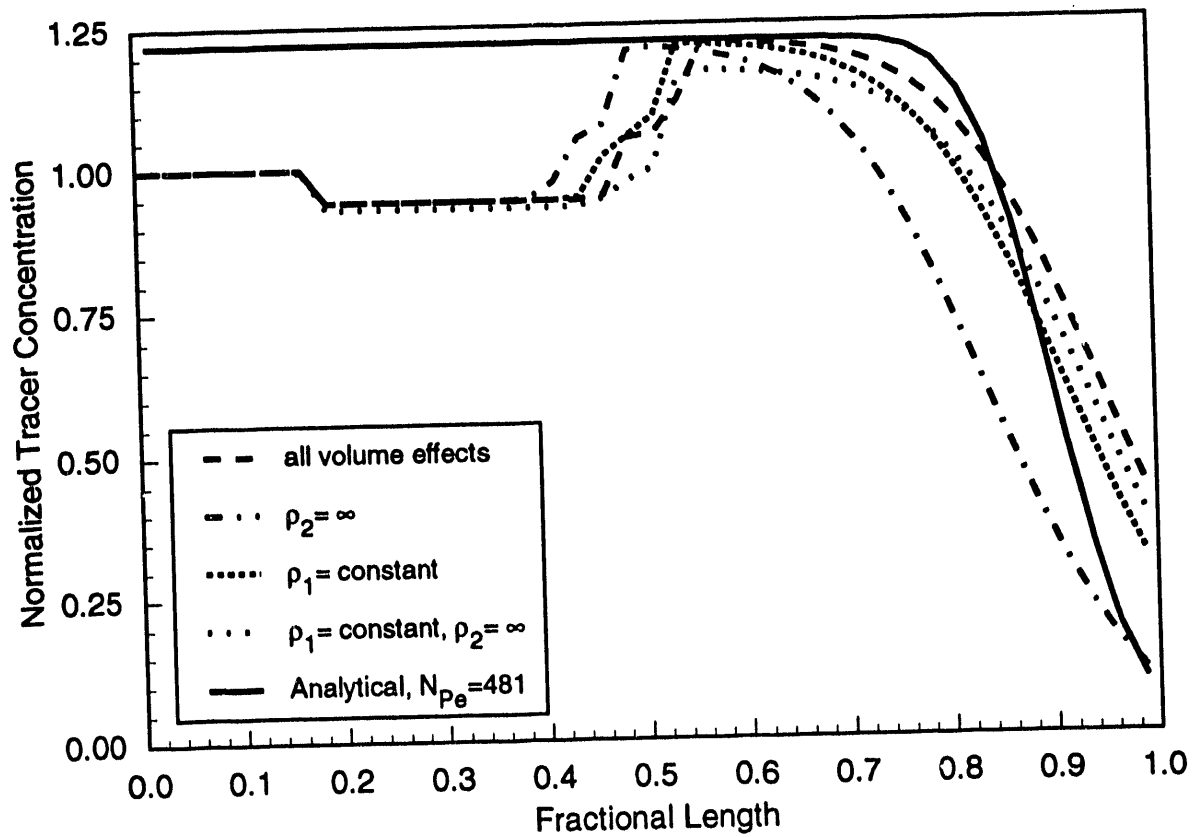
Figure 3. Aqueous tracer concentration T(aq) at $t=1.8 \times 10^5$ seconds, as a function of different volume assumptions.
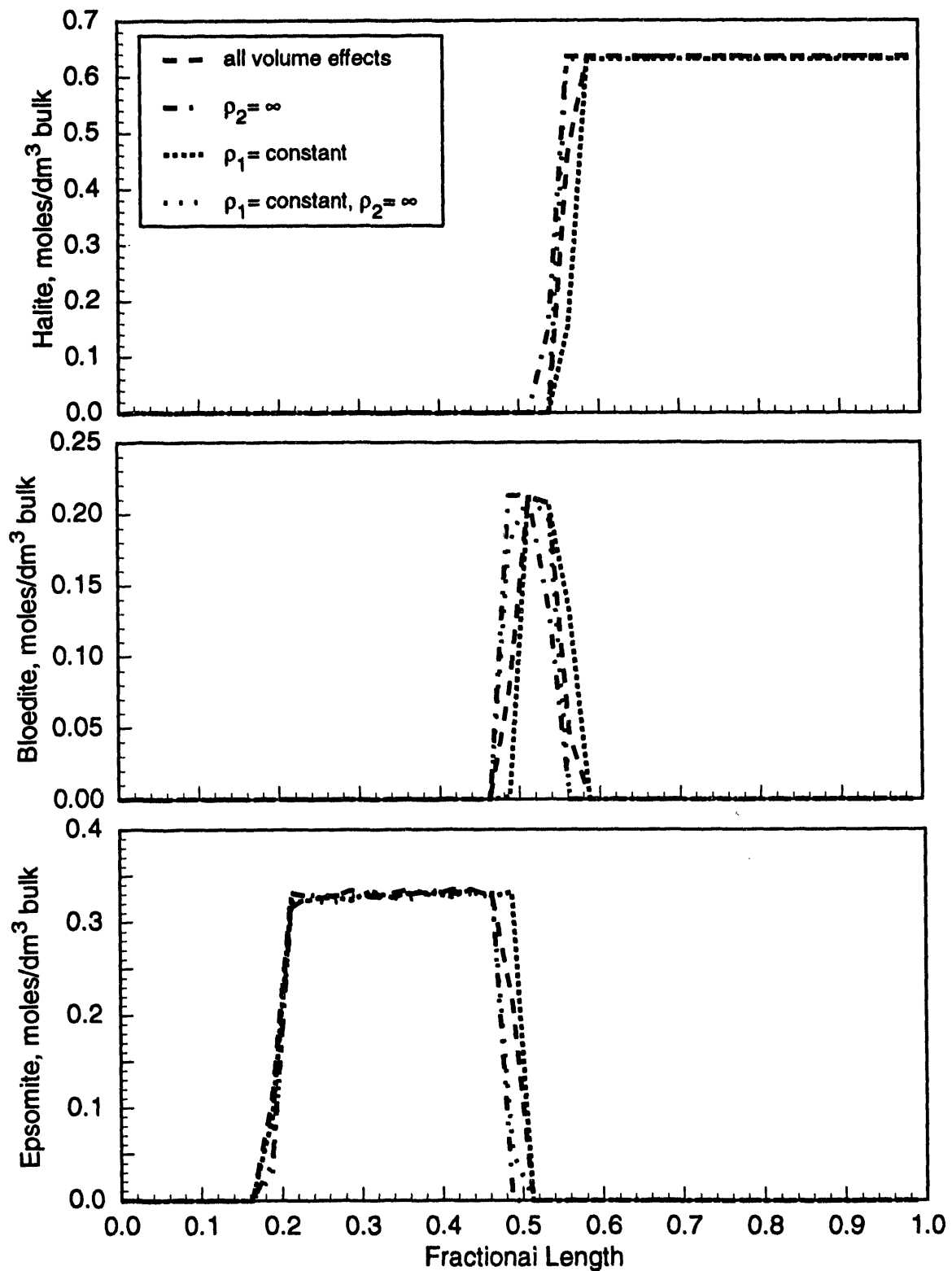
Figure 4. Slight variation in position of mineral dissolution/precipitation fronts at $t=1.8 \times 10^5$ seconds, as a function of different volume assumptions.

END

DATE FILMED
2 / 8 / 94